AIP | Review of Scientific Instruments

Far-infrared ellipsometer

K.-L. Barth and F. Keilmann

Citation: Review of Scientific Instruments **64**, 870 (1993); doi: 10.1063/1.1144135
View online: http://dx.doi.org/10.1063/1.1144135
View Table of Contents: http://scitation.aip.org/content/aip/journal/rsi/64/4?ver=pdfcov
Published by the AIP Publishing

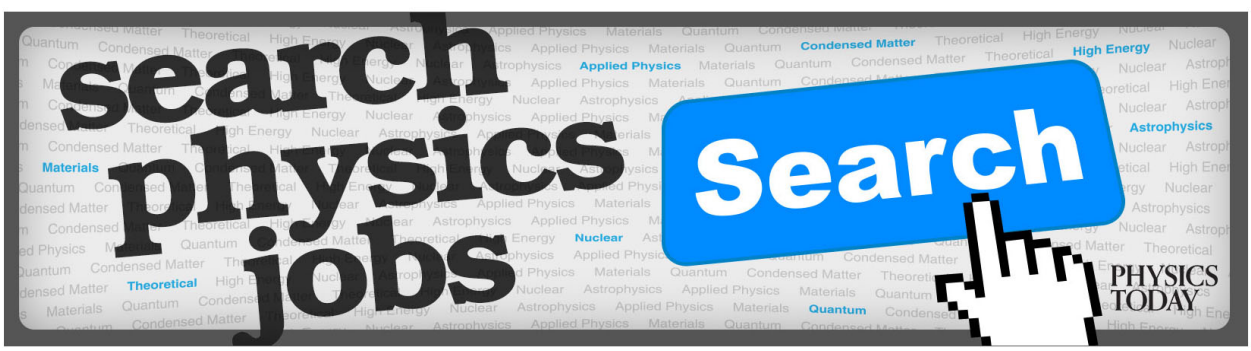

Far-infrared ellipsometer

K.-L. Barth and F. Keilmann
Max-Planck-Institut für Festkörperforschung, Heisenbergstrasse 1, 7000 Stuttgart 80, Germany

(Received 28 September 1992; accepted for publication 2 December 1992)

A far-infrared rotating-analyzer ellipsometer which uses a step-tunable, optically pumped gas laser as its light source is described herein. As polarizers novel metal grids with 10 000:1 polarization contrast were used. The instrument determines the complex dielectric function in the spectral range between 10 and 150 cm^{-1}. A cryostat allows both reflection and transmission measurements from 10 to 330 K. Measurements of the birefringence of crystalline quartz, of both the carrier density and the scattering frequency of doped semiconductors, and of the low energy excitations of high-T_C YBaCuO ceramics are presented herein.

I. INTRODUCTION

Ellipsometry[1–6] is a powerful technique in nondestructive and contactless material characterization. Typical applications are to determine optical properties of surfaces and to measure the thickness of surface layers or thin films. Ellipsometric instrumentation is well developed in and near the visible spectral region.

The main advantage of *spectroscopic* ellipsometry is the possibility to determine both optical constants without the need to perform a Kramers–Kronig analysis. Furthermore, no reflection standard is required, in contrast to common reflectometry. Finally, scattering losses due to macroscopic surface roughness give only minor disturbance.

In recent years efforts were made to extend ellipsometry into the ultraviolet[7] and the infrared spectral regions.[8–10] The far-infrared has seen only few approaches[11] although there is a strong interest in methods which can measure the optical constants in this region. Note, for example, that high-T_C superconductors and heavy Fermion metals have material properties that are not understood but may well be explained by far-infrared excitations. Unfortunately these materials show very high reflectivity especially in the far-infrared, and therefore methods like Fourier-transform spectroscopy become quite insensitive. Our approach to build a far-infrared rotating-analyzer ellipsometer (RAE), to our knowledge the first of its kind, presents a new alternative to studying these materials.

This article describes the setup of the ellipsometer and discusses the sensitivity and limitations of the instrument. Three examples of applications are given.

II. PRINCIPLE OF MEASUREMENT

An ellipsometer basically consists of a monochromatic light source, a linear polarizer, the sample to be investigated, a linear analyzer (a second linear polarizer), and a detector. Ellipsometric measurements monitor the change in polarization state of light reflected from the sample surface. This can be done in different ways, for example, with a rotating analyzer,[12–16] a method pioneered by Aspnes.[17] This RAE, in contrast to null ellipsometers,[2,3] allows an automation of the measuring procedure for rapid determination of the optical spectra. RAEs avoid the use of a compensator which by its strong wavelength dependence would constrict the spectral range of the ellipsometer.

In ellipsometry linearly polarized light is incident under an oblique angle onto the surface under investigation. The reflected light is, in general, elliptically polarized. This is due to the fact that the Fresnel reflection coefficients r_p (for E parallel to the plane of incidence) and r_s (E perpendicular) are different. Ellipsometry determines the complex ratio

$$\rho=\frac{r_p}{r_s}=\tan\psi e^{i\Delta},\quad \tan\psi=\frac{|r_p|}{|r_s|},\quad \Delta=\delta_{r_p}-\delta_{r_s} \tag{1}$$

by measuring the ellipsometric angles ψ and Δ. The reflection coefficients depend on the angle of incidence, the material properties, and therefore also on the wavelength. Aspnes[2] showed that optimum sensitivity of a RAE requires the angle of incidence to be as close as possible to the "principal angle" ϕ_p given by $\Delta(\phi_p)=\pi/2$. As a consequence, different geometrical arrangements are required to obtain the best sensitivity from an ellipsometer in different spectral regions and for different classes of materials. Our far-infrared ellipsometer is planned for highly reflecting materials. Theoretical calculations[16] then call for nearly grazing incidence. There is however a conflict for limited sample sizes. We have chosen angles of incidence between 70° and 80°.

III. INSTRUMENT SETUP

The design of our RAE has to take into account the special conditions of the far-infrared frequency region. As a main point the long wavelengths require diffraction effects to be included in the optical layout.

Figure 1 shows a sketch of our far-infrared RAE. The light source is an optically pumped far-infrared laser with plane cavity mirrors (model 195 FIR, Edinburgh Instruments Ltd.). The output beam is coupled through a 5 mm central hole and has a power of about 1 mW. The laser provides a large number of discrete frequencies[18–22] in the range from about 7 up to 2000 cm^{-1}. To operate the laser we choose the appropriate gas (mostly one of the isotopic variety of methyl alcohols) and optimize the resonator length for one of several possible lines. Although there exist sufficient lines for measuring quasicontinous spectra, it is often difficult to find a special frequency with appropriate stability and intensity.

 0034-6748/93/040870-06$06.00

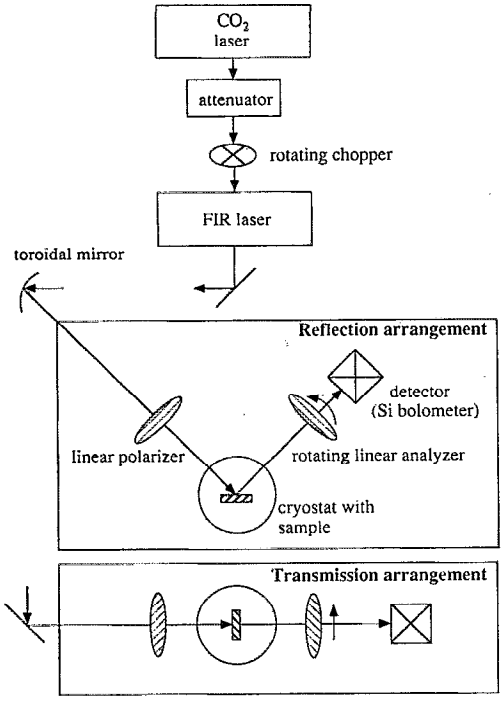

FIG. 1. Setup of the far-infrared laser ellipsometer.

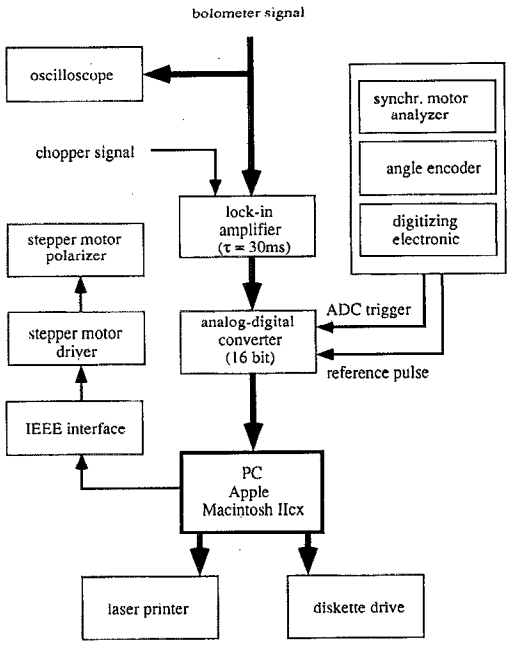

FIG. 2. Block diagram of the ellipsometer electronics. A computer controls the position of the polarizer and reads out detector signals and corresponding angular positions of the analyzer.

Beam propagation is approximated by Gaussian optics.[23–25] We recollimate the emerging beam after 63 cm travel distance with a toroidal mirror (f_{eff}=460 mm) used at 35° incidence angle. The collimated region is situated at a distance near 164 cm from the mirror for all far-infrared frequencies. Here we place the linear polarizer, the cryostat, and the rotating linear analyzer, and thus have a common optical setup for all wavelengths of interest.[16] With this arrangement the beam waists are characterized by confocal parameters between 24 cm (at 10 cm^{-1}) and 123 cm (at 100 cm^{-1}) at beam diameters of about 12 mm. This results in a small beam convergence of 0.7° at 10 cm^{-1} and a small beam divergence of 0.2° at 100 cm^{-1}.

Far-infrared polarizers usually consist of an array of free standing wires of small diameter which are arranged in close periodicity.[26–28] With these elements a polarization contrast of about 1:0.003 (transmittance with electric field perpendicular and parallel to the wires, respectively) can be achieved. Other designs have used fine strip gratings on dielectric films[29] also with nonsatisfactory polarization contrast. In our ellipsometer we apply for the first time new strip-grating-type polarizers with a polarization contrast better than $1:10^{-4}$ (model P 01, INFRASPECS, Poststrasse 32, D-7024 Filderstadt 4, Germany). They consist of a transparent substrate material such as polyethylene or Kapton with a periodic array of gold stripes of a special geometry. The gold stripes have a thickness (measured in the direction of the laser beam) equal to the distance between stripes, such that a short channel is formed which acts as a cutoff waveguide for the polarization to be rejected. The polarizer is mounted on a plane metal ring and connected with a rotary table (UR 80 MS, Spindler und Hoyer). One unit is used as polarizer and driven by a stepping motor (KP 6 AM 2/008 1.8°/step, Japan Servo Co. Ltd.) with resolution 0.0025°. The other, used as analyzer, is driven by a synchronous motor (RSM 64/4 NG 750 U/min, Berger Lohr) and rotates at 0.347 Hz. The analyzer rotary table is connected to an angular encoder (Inkrementaldrehgeber ERO 725, Heidenhain) which gives 36 000 pulses plus one reference pulse per rotation. The signals of the encoder are digitized (EXE 602, Heidenhain) and used to trigger the data acquisition. The analyzer azimuth can thus be determined with an accuracy of about 0.01°.

The cryostat is a commercial, cold-finger-type (Konti–Cryostat Spektro A/So, Cryovac) and allows measurements in a temperature range between 3.6 and 330 K. The temperature is controlled manually (TIC303 M, Cryovac). The cryostat has two 30-mm-diam windows, about 50 mm from the sample, for reflection measurements at an angle of incidence of 80°. As window material we use a 15 μm thick mylar foil. The influence of the foils on the state of polarization ($<1°$ in Δ and $<0.3°$ in ψ) is smaller than the relative error bar and therefore can be neglected. The cryostat unit is mounted on a rotary table, the angular position can be determined to $\pm 1/60°$.

The reflected beam is focused with a lens on a silicon bolometer (Infrared Laboratories Inc.). The detector has a high responsivity ($S=3.85\times10^5$ V/W) and low noise [noise equivalent power (NEP)$=2.75\times10^{-13}$ W/$\sqrt{\text{Hz}}$] in a spectral region between 5 and 1500 μm. At a fixed amplifier setting the detection system is linear over a range exceeding four orders of magnitude, a necessary condition for rotating-analyzer ellipsometry.

The output of the detector is amplified by a lock-in amplifier for further treatment in a computer. The use of lock-in techniques in ellipsometry[30] has the advantage that

the signal zero is exactly defined, and therefore, further calibration steps[12–14] can be avoided.

IV. MEASUREMENT PROCEDURE

Data acquisition and data reduction of our far-infrared RAE is computer controlled (Macintosh IIcx) using LabVIEW (National Instruments) software. The computer actively controls the position of the polarizer, reads out the power signal and analyzer positions, and calculates the ellipsometric angles and the complex dielectric function (see Fig. 2).

When the analog-to-digital (AD) converter (NB-MIO-16, National Instruments) gets the reference pulse from the angle encoder, 360 AD conversions are initiated (every 100th trigger pulse from the encoder is used for an AD conversion). This results in 360 data points per turn of the analyzer. The far-infrared laser power exhibits a slow drift in times $\tau \gg 3$ s and also fast fluctuations with $\tau \ll 3$ s. We have chosen to average over 50 rotations at a frequency of 0.347 Hz to average over the fluctuations. Thus the time Δt between two consecutive AD conversions is 8 ms. For optimum signal-to-noise ratio the time constant of the signal electronic τ_e should be several times the interval Δt.[17] When we choose the time constant of the lock-in to be 30 ms, this relation is fullfilled reasonably well.

The detected power S can be expressed as the second harmonic of a Fourier expansion[31]

$$S(A_i) \sim 1+\alpha(\rho,P)\cos 2A_i+\beta(\rho,P)\sin 2A_i . \tag{2}$$

A_i is the angular position of the analyzer at the ith data point,

$$A_i=\frac{2\pi(i-1)}{N}, \quad i=1,...,N. \tag{3}$$

P is the angular position of the polarizer, α and β are normalized Fourier coefficients which depend on P and the complex ratio of the Fresnel coefficients ρ [see Eq. (1)]. With Eqs. (1) and (2) we can express the ellipsometric angles ψ and Δ in terms of the Fourier coefficients α and β:

$$\tan\psi=\sqrt{\frac{1+\alpha}{1-\alpha}}\tan P, \tag{4}$$

$$\cos\Delta=\beta/\sqrt{1-\alpha^2}. \tag{5}$$

The coefficients α and β are determined by the measured power values $S(A_i)$:[17]

$$\alpha=\left[2\sum_{i=1}^{N} S(A_i)\cos 2A_i\right] \Big/ \left[\sum_{i=1}^{N} S(A_i)\right], \tag{6}$$

$$\beta=\left[2\sum_{i=1}^{N} S(A_i)\sin 2A_i\right] \Big/ \left[\sum_{i=1}^{N} S(A_i)\right]. \tag{7}$$

The determination of the coefficients α and β is sensitive to the absolute calibration of the polarizer and analyzer angles, and also to electronic distortions of the power signal. The pertinent calibration procedure is discussed below.

For one wavelength the measuring procedure and the computation of the optical constants takes about 160 s.

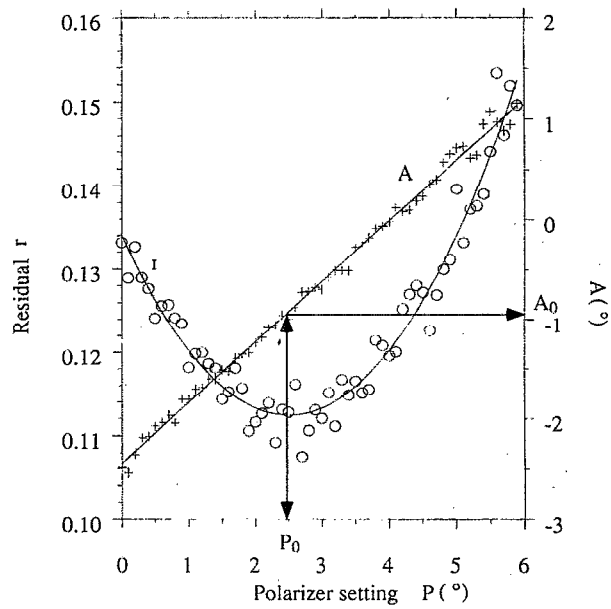

FIG. 3. Calibration of the ellipsometer using an absorbing Si sample in reflection: the residual r and the angle A are measured at different polarizer settings P. Fits to r and A then determine the true zero settings, P_0 and A_0, respectively, of the polarizer and analyzer scales, and the parameter η.

V. CALIBRATION OF THE ELLIPSOMETER

The classical "residual" calibration method is discussed in Refs. 17 and 31. Basic to this method is that linearly polarized light incident at oblique angle onto an absorbing medium is reflected purely linearly, polarized only when the polarization lies *in* the plane or *perpendicular* to the plane of incidence. The procedure consists of measurements of the coefficients α and β with polarizer settings P near one of these positions.

The residual

$$r(P)=1-\alpha^2-\beta^2 \tag{8}$$

then is a measure for the deviation of the reflected polarization state from linear. It shows a minimum when the polarizer orientation is in the plane of incidence. α and β are the measured Fourier coefficients. A typical result of such a calibration procedure of the far-infrared ellipsometer at 61.34 cm^{-1} is shown in Fig. 3. We used n-Si as sample material. We determine $P_0=2.45\pm0.1°$ as the absolute zero position of the polarizer. The minimum residual exceeds zero since the power signal is distorted in the detection and amplification process. The minimum value of r at P_0 defines the attenuation factor:[17,31]

$$\eta=1/\sqrt{1-r_{\min}}, \tag{9}$$

which directly corrects any measured Fourier coefficients for distortion in the detection system.

The calibration values of α and β at P_0 are likewise used to obtain A_0, the zero position of the analyzer,[13,14,16] using

$$A(P)=-\tfrac{1}{2}\arctan(\beta/\alpha). \tag{10}$$

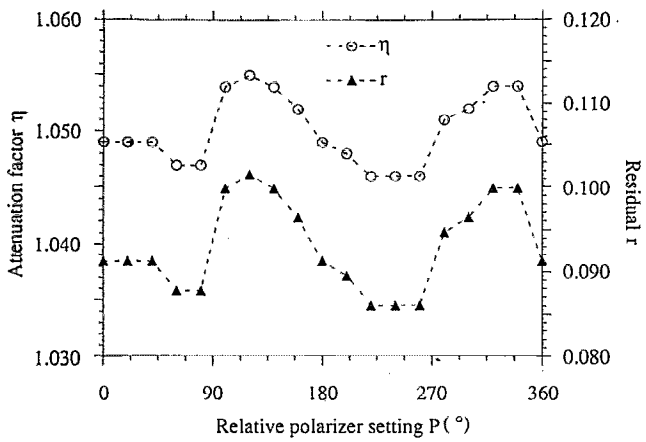

FIG. 4. Experimentally determined dependence of η (left scale) and r (right scale) on the polarizer angle P. η and r show a small polarization dependence of the detection system which could be reduced to about 3%.

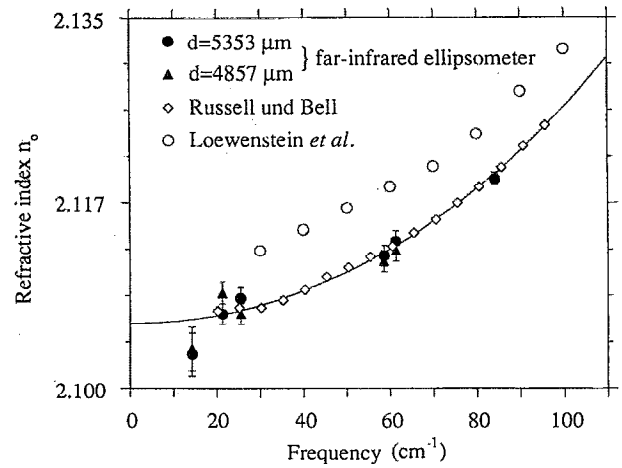

FIG. 5. Refractive index n_o of quartz (ordinary ray) vs far-infrared frequency. The ellipsometric data agree with the results of Refs. 36 and 37. The solid line is a calculation after Ref. 37.

The theory curves in Fig. 3 are from parabolic fits to Eqs. (8) and (10). Note that $A_0=-0.9\pm0.2°$ obtained in this way contains the corrections for the scale offset and the electronic phase shift due to the time constant of the detection system.

The sensitivity of the residual method depends on the curvature of the residual curve $r(P)$. This curvature increases with increasing sample absorption,[17,31] thus the residual method is limited to strongly absorbing material. A different calibration method based on a phase effect is useful with weakly absorbing materials.[32]

A simple polarizer-analyzer-detector configuration without sample was used to test linearity and polarization isotropy of the detector. A nonlinearity of the detector was not observable. We measured r at different polarizer settings P between 0° and 360° in steps of 10°. Since the radiation stays linearly polarized, r [and from Eq. (9) η] should ideally be independent of P. In Fig. 4 we show the result at a frequency of 61.34 cm^{-1}. η is constant to within 3% only. This represents, however, a factor of 5 improvement which we achieved by modifying the detector: we removed the Winston cone[33] and the quartz filter, to avoid their polarization effects. Also we mounted the Si bolometer on the back surface of the diamond heat sink to avoid polarizing effects of the lead wires. Lastly we placed absorbing apertures along the beam path. The remaining oscillatory variation of r and η is seen to increase with wavelength, probably due to increasing diffraction effects.

Russev describes a method to correct the influence of nonlinear and polarization-dependent detector characteristics on the determination of the Fourier coefficients.[34] This method requires a reproducible $r(P)$ behavior. Unfortunately in our case $r(P)$ turns out to be unreproducible on each new alignment and thus we could not apply the procedure for practical reasons.

To test the polarization independence of the detection system in the reflection ellipsometry configuration (polarizer–reflecting sample–analyzer) we have to reflect from a nonpolarizing mirror. Calculations[16] show that up to an angle of incidence of 80° we can use a silver mirror for this purpose. Monitoring $r(P)$ with the silver mirror as sample we could align for minimum polarization dependence of the detection system. From $\eta(P)$ at the optimum setting we determine the uncertainty $\Delta\eta$ which we use to calculate the error bar of the dielectric function (see below).

VI. APPLICATIONS

In a first application of the instrument we studied a known birefringent material, natural crystalline quartz. The optical constants $N_o=n_o+ik_o$ and $N_e=n_e+ik_e$ of the ordinary and extraordinary rays, respectively, have been measured before.[35–37]

We used the ellipsometer in a simple transmission configuration and measured the phase shift between orthogonal components passing through a plane parallel plate. The change of polarization of linearly polarized coherent light passing through a plane parallel anisotropic plate is given in the literature.[38–41]

From the measured phase shift we calculate the refractive index n_o of the ordinary ray by taking n_e from the literature and setting $k_o=k_e=0$. The result is shown in Fig. 5. For two plate thicknesses ($d_1=5353\pm1$ μm, $d_2=4857\pm1$ μm) we obtain fair agreement, especially at higher frequencies. The larger discrepancy at lower frequencies probably comes from the polarization anisotropy of the detector which is more pronounced at low frequencies. Our data agree with the results of Russell *et al.*[36] (and Passchier *et al.*,[37] for reasons of clarity not shown in the figure). The results of Loewenstein *et al.*,[35] by contrast, differ substantially by more than our estimated error.

In the following the ellipsometer is used in the reflection configuration. We demonstrate the measurement of the dielectric function of n type Si. Using the Drude model (see, for example, Ref. 42) we can determine both quantities of interest, carrier density n_e and scattering frequency ω_τ with a measurement at one single frequency. Using far-infrared frequencies then has two advantages: there are no lattice vibration contributions at $\lambda\geqslant100$ μm which

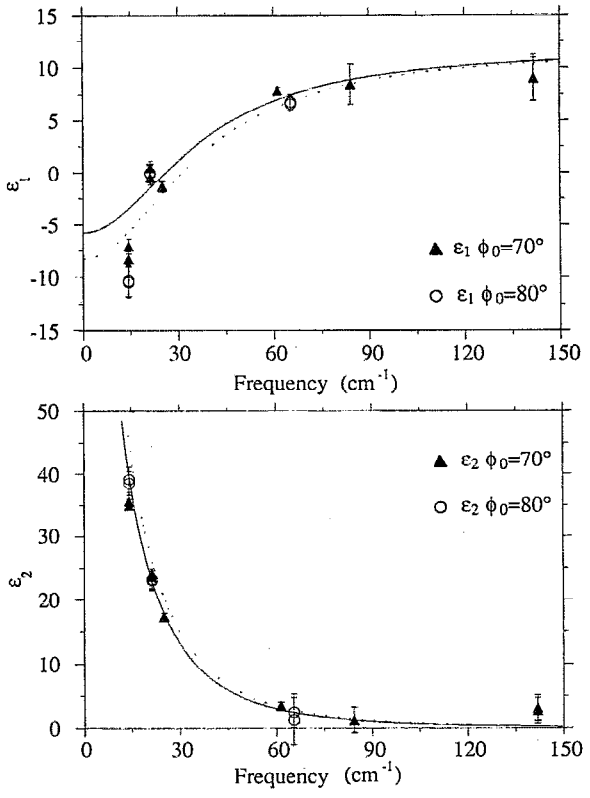

FIG. 6. Ellipsometrically determined dielectric function of Si:P vs frequency, at two different angles of incidence. The experimental results are fitted with the Drude model ($n_e=7\times10^{16}$ cm^{-3}, $\omega_\tau=7\times10^{12}$ s^{-1}). The dotted curve demonstrates what to expect with a 10% increase of the carrier density.

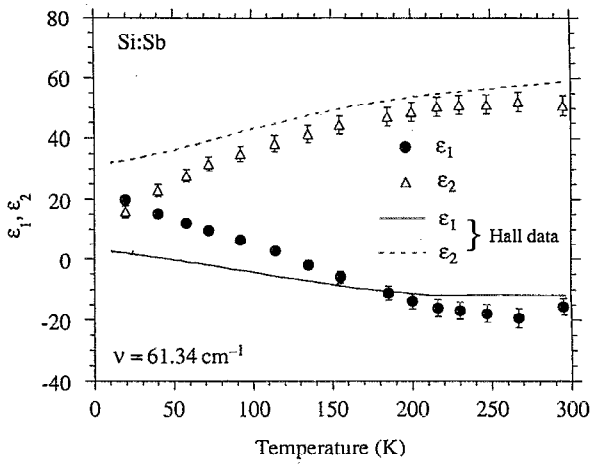

FIG. 7. Dielectric function of Si:Sb vs temperature, ellipsometrically determined at a frequency of 61.34 cm^{-1}. The lines are the results of a Hall measurement.

could interfere with the analysis, and there is a sizable free carrier absorption which makes the measurement very sensitive.

Calculations[16] show that far-infrared RAE measurements on semiconducting material can best resolve carrier densities between $n_e=10^{16}$ and 10^{18} cm^{-3}, requiring angles of incidence between 70° and 80°.

In Fig. 6 we show the results of measurements on Si:P at two different angles of incidence. The real and imaginary parts of the dielectric function show the expected Drude-like behavior. A fit (solid lines) results in $n_e=7\times10^{16}$ cm^{-3} and $\omega_\tau=7\times10^{12}$ s^{-1}. To illustrate the sensitivity of the method, we show a calculated curve for a 10% increase of the carrier concentration n_e (dotted). At 70° angle of incidence the sensitivity peaks at about 60 cm^{-1}, since here Δ is about 90°. With the measured dielectric function at this frequency we get $n_e=(1.7\pm0.12)\times10^{17}$ cm^{-3} and $\omega_\tau=(1.1\pm0.11)\times10^{13}$ s^{-1}. These results are in fair agreement with the specifications of the supplier: $n_e=(8$–$10)\times10^{16}$ cm^{-3} and $\omega_\tau=(9$–$12)\times10^{12}$ s^{-1}. In principle any pair of ϵ_1 and ϵ_2 values can be used to determine n_e and ω_τ. Ellipsometer sensitivity, however, becomes poor for frequencies substantially detuned from 60 cm^{-1}, at a 70° angle of incidence. In this case the error bars for n_e and ω_τ increase. At low frequencies diffraction effects cause an additional systematic error. This is probably the reason for the strongly deviating result at 14 cm^{-1}.

In a further experiment we have measured the temperature dependence of the complex dielectric constant of Si:Sb at 61.34 cm^{-1}. An angle of incidence of 80° was chosen to optimize sensitivity. The results of this measurement (Fig. 7) show relatively small scatter but deviate markedly from the Hall data. We believe that this is an artifact in the ellipsometer, probably due to small changes in the angle of incidence coming from mechanical contraction in the cryostat during the cooling procedure. This could in principle be avoided by monitoring the angle with an appropriate method, for example, with a HeNe laser.

In Fig. 8 we show the results of a first application of the method to high-T_C material. We used a sintered ceramic of $YBa_2(Cu_{1-c}Fe_c)_3O_{7-\delta}$ with an iron concentration of $c=2\%$ and $\delta\approx0$. Iron is known to induce a spectral structure at far-infrared frequencies which can be interpreted as an energy gap (for a detailed description see Ref. 43). Only small sample diameters of 10 mm were available and thus diffraction leads to systematic errors at frequencies below 60 cm^{-1}.[16] Above 60 cm^{-1} our ellipsometric data show a clear frequency and temperature behavior which is in qualitative agreement with Fourier-transform measurements on the same sample from Seider *et al.*[44–46] The frequency dependence of the dielectric function shows a Drude-like behavior. The real part of the dielectric function reaches large negative values for low temperatures, an indication that the sample gets superconducting. ϵ_2 does not reach zero for decreasing frequencies and low temperatures as would be expected according to Bardeen–Cooper–Schrieffer theory for a perfect superconductor below the gap frequency. This may indicate a large normal conduction part contributing to the dielectric function.

VII. DISCUSSION

We estimate the error with which we can determine the complex dielectric function. The decisive uncertainties are in the angle of incidence $\Delta\phi_0$ and in the parameters ΔP_0, ΔA_0, and $\Delta\eta$ used to calibrate the instrument. The dominating error in our far-infrared configuration results

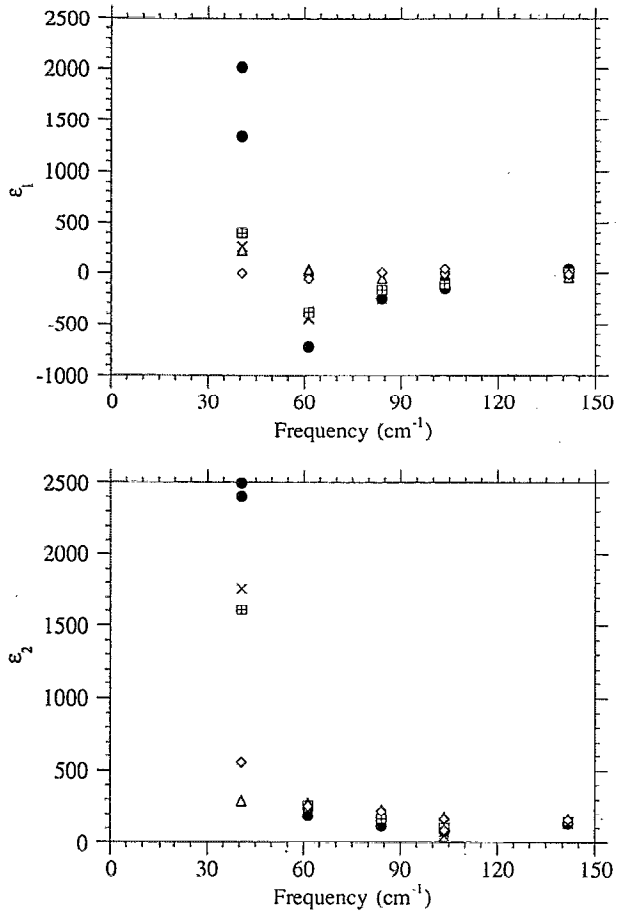

FIG. 8. Dielectric function of a 2% Fe doped YBaCuO ceramic (● 14 K, × 49 K, ⊕ 67 K, △ 125 K, ◇ 296 K).

from $\Delta\eta$ which we could not reduce below about 3% (see Fig. 4) due to the unreproducible polarization anisotropy of the detection system. With $\Delta P_0 = \pm 0.1°$, $\Delta A_0 = \pm 0.2°$, and $\Delta\eta = \pm 0.015$ we calculate largest errors of several degrees for the ellipsometric angles ψ and Δ, which results in uncertainties of about 10% in the complex dielectric function (see also Ref. 2).

A conceivable improvement of the instrument could be the replacement of the light source: a tunable *p*-Ge laser or a free electron laser as the light source would allow measurements of continuous spectra.

Further experiments with high-T_C materials are in progress. They benefit from the advantage of the method that the dielectric function can be determined relatively quickly. This provides access to time-dependent effects on a minute time scale to be reported elsewhere.

ACKNOWLEDGMENTS

We would like to thank D. Böhme, K.-W. Kussmaul, and W. Schlieter for expert technical assistance.

[1] R. M. A. Azzam and N. M. Bashara, *Ellipsometry and Polarized Light* (North-Holland, Amsterdam, 1977).
[2] D. E. Aspnes, in *Optical Properties of Solids: New Developments*, edited by B. O. Seraphin (North-Holland, Amsterdam, 1976), Chap. 15, p. 800.
[3] D. E. Aspnes, in *Handbook of Optical Constants of Solids*, edited by E. D. Pallik (Academic, New York, 1985), Chap. 5, p. 85.
[4] *Proceedings of the Symposium on Recent Developements in Ellipsometry*, edited by N. M. Bashara, A. B. Buckman, and A. C. Hall (North-Holland, Amsterdam, 1976).
[5] R. H. Muller, Surf. Sci. **16**, 14 (1969).
[6] P. S. Hauge, Surf. Sci. **96**, 108 (1980).
[7] R. L. Johnson, J. Barth, M. Cardona, D. Fuchs, and A. M. Bradshaw, Rev. Sci. Instrum. **60**, 2209 (1989).
[8] F. Ferrieu, Rev. Sci. Instrum. **60**, 3212 (1989).
[9] A. Röseler, *Infrared and Spectroscopic Ellipsometry* (Akademie, Berlin, 1990).
[10] J. Bremer, O. Hunderi, Kong Fanping, T. Skauli, and E. Wold, SINTEF Report, No. STF19 A91004, Foundation for Scientific and Industrial Research at the Norwegian Institute of Technology.
[11] R. O. DeNicola, M. A. Saifi, and R. E. Frazee, Appl. Opt. **11**, 2534 (1972).
[12] L. Vina Liste, Dissertation, Universität Stuttgart, 1984.
[13] P. Lautenschlager, Dissertation, Universität Stuttgart, 1987.
[14] M. Garriga Bacardi, Dissertation, Universität Stuttgart, 1990.
[15] S. Zollner, Dissertation, Universität Stuttgart, 1991.
[16] K.-L. Barth, Dissertation Universität Stuttgart, 1991.
[17] D. E. Aspnes and A. A. Studna, Appl. Opt. **14**, 220 (1975).
[18] N. G. Douglas, *Millimetre and Submillimetre Wavelength Lasers*, Springer Series in Optical Sciences, Vol. 61 (Springer, Berlin, 1989).
[19] M. Inguscio, J. Appl. Phys. **60**, 178 (1986).
[20] D. J. E. Knight, National Physics Laboratory, Teddington, NPL Report No. Qu 45, 1981.
[21] N. Rosenbluh, R. J. Temkin, and K. J. Button, Appl. Opt. **15**, 2635 (1976).
[22] Y. Tsunawaki, M. Yamanaka, and S. Kon, Rev. Laser Eng. **10**, 78 (1982).
[23] H. Kogelnik and T. Li, Appl. Opt. **5**, 1550 (1966).
[24] A. E. Siegman, *An Introduction to Lasers and Masers* (McGraw-Hill, New York, 1971).
[25] S. Solimeno, B. Crosignani, and P. Di Porto, *Guiding, Diffraction, and Confinement of Optical Radiation* (Academic, New York, 1986).
[26] H. Du Bois and H. Rubens, Wied. Ann. **46**, 542 (1892).
[27] W. G. Chambers, T. J. Parker, and A. E. Costley in, *Infrared and Millimeter Waves*, edited by K. J. Button (Academic, New York, 1986), Vol. 16, p. 77.
[28] H. Hertz, Wied. Ann. **36**, 769 (1889).
[29] W. A. Challener, P. L. Richards, S. C. Zilio, and H. L. Garvin, Infrared Phys. **20**, 215 (1980).
[30] B. D. Cahan and R. F. Spanier, Surf. Sci. **16**, 108 (1969).
[31] D. E. Aspnes, J. Opt. Soc. Am. **64**, 812 (1974); corrections in, D. M. Radman and B. D. Cahan, *ibid.* **71**, 1564 (1981).
[32] J. M. M. de Nijs, A. H. M. Holtslag, A. Hoeksta, and A. van Silfhout, J. Opt. Soc. Am. A **5**, 1466 (1988).
[33] D. A. Harper, R. H. Hildebrand, R. Stiening, and R. Winston, Appl. Opt. **15**, 53 (1976).
[34] S. H. Russev, Appl. Opt. **28**, 1504 (1989).
[35] E. V. Loewenstein, D. R. Smith, and R. L. Morgan, Appl. Opt. **12**, 398 (1973).
[36] W. F. Passchier, D. D. Honijk, M. Mandel, and M. N. Afsar, J. Phys. D: **10**, 509 (1977).
[37] E. E. Russell and E. E. Bell, J. Opt. Soc. Am. **57**, 341 (1967).
[38] H. Melle, Optik **65**, 115 (1983).
[39] K. Zander, H. Melle and J. Moser, Physikalisch-Technische Bundesanstalt, Abteilung Optik, PTB-OPT-14, ISSN 0341-6712, Braunschweig, 1983.
[40] K. Zander, J. Moser and H. Melle, Optik **70**, 6 (1984).
[41] E. Gerstenhauer and R. Thomas, DPG (VI) **13**, 130 (1978).
[42] P. Grosse, *Freie Elektronen in Festkörpern* (Springer, Berlin, 1979).
[43] M. Bauer, Dissertation, Universität Tübingen, 1990.
[44] E. Seider, Dissertation, Universität Stuttgart, 1991.
[45] E. Seider, M. Bauer, L. Genzel, P. Wyder, A. Jansen, and C. Richter, Solid State Commun. **72**, 85 (1989).
[46] E. Seider, M. Bauer, L. Genzel, and H.-U. Habermaier, Z. Phys. B: **83**, 1 (1991).